System Z_{DR} of the WSR-88D: Hardware Issues and Temperature Dependence

Valery Melnikov[1,2], Dusan Zrnic[2], Alan Free[3,4], Richard Ice[3,4], and Robert Macemon[3,4]

[1] – *CIMMS, the University of Oklahoma, Norman, Oklahoma*

[2]- *NOAA/OAR National Severe Storms Laboratory, Norman, Oklahoma*

[3] – *Centuria Corporation.*

[4]- *NOAA/NWS Radar Operations Center, Norman, Oklahoma.*

1. Introduction

Quantitative precipitation estimates require accurate measurements of reflectivity (Z) and differential reflectivity (Z_{DR}). Accurate measurements of Z_{DR} depend on its calibration, i.e., obtaining the system Z_{DR} (Z_{DR}sys) sometimes also called system Z_{DR} bias. According to the WSR-88D's specifications, Z_{DR}sys should be obtained with accuracy of 0.1 dB. The RF parts of radar hardware: the antenna, waveguides, couplers, circulators, power divider, and low noise amplifiers (LNA) introduce different amplifications/attenuations in the H- and V-channels that are the sources of Z_{DR} bias. The IF (intermediate frequency) digitizer (IFD) may also contribute to Z_{DR}sys (Fig. 1). The signal processor RVP is a measurement device.

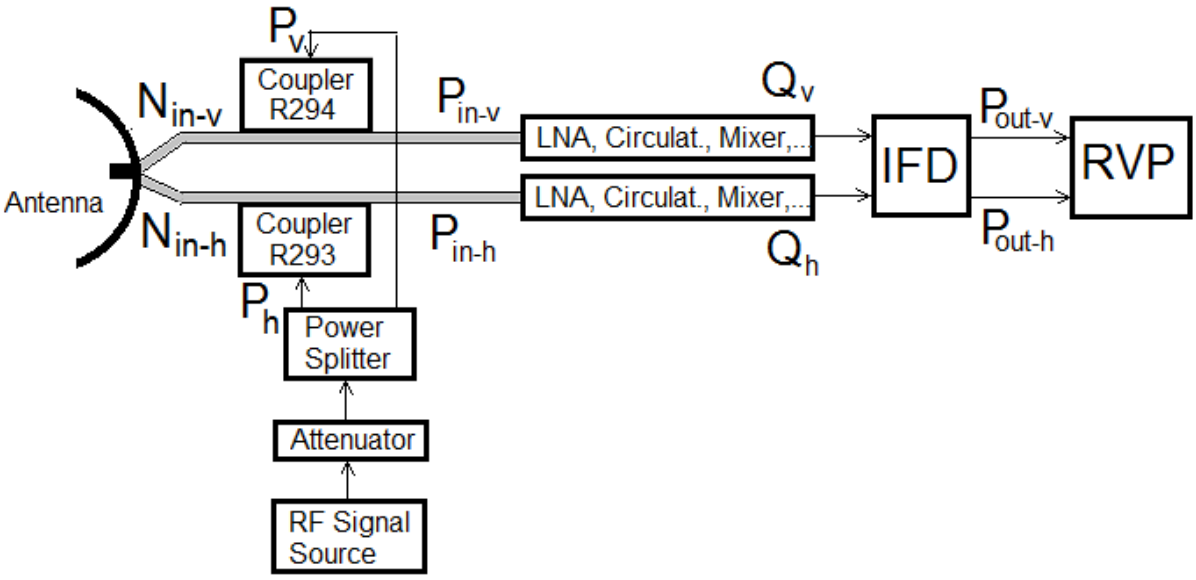

Fig. 1. Diagram of receiver calibration. The waveguides are shown with thick shadowed lines.

To obtain Z_{DR}sys, the WSR-88Ds have dedicated hardware and software to perform the base-line engineering calibration. We present results of measurements of the H- and V-channel amplifications contributing to Z_{DR}sys. To separate the contributions to Z_{DR}sys introduced by radar hardware and IFD, two types of measurements have been

conducted. First, signal matching was measured using the built-in signal source (a part of the radar calibration hardware) as it is shown in Fig. 1. In this measurement the mismatch of the radar hardware and IFD was measured. Second, the external calibrated generator was connected to the input to IFD to measure the signal mismatch in the IFD. Three radars were used in the measurements: KJIM, KREX, and KOUN. The first two have no antenna and KOUN is a full WSR-88D radar. Note that the antenna was not involved in the measurements presented in here. In terms of the WSR-88D calibration, this procedure required obtaining the receiver bias (RCB) contribution to Z_{DR}sys.

Z_{DR} can be calculated from measured signal-to-noise ratio (SNR) or from the measured powers in the horizontal and vertical radar channels. Below, Z_{DR} calculations from the SNR are discussed. The noise powers N_h and N_v in the horizontal (hereafter H) and vertical (hereafter V) polarization channels were measured by the digital subsystem before injecting CW test signal. The SNR levels were calculated in two forms. The first is

$$SNR_{hn} = 10 \log(P_h/N_h) \quad \text{and} \quad SNR_{vn} = 10 \log(P_v/N_v), \tag{1}$$

i.e., no noise correction is done to the input powers, where P_h and P_v are the measured signal powers in the channels, and subscripts hn and vn indicate no noise correction. The second form is noise corrected SNR:

$$SNR_h = 10 \log[(P_h - N_h)/ N_h] \quad \text{and} \quad SNR_v = 10 \log[(P_v - N_v)/ N_v], \tag{2}$$

By definition, Z_{DR} is a ratio of the pure weather powers and should be calculated as the ratio of the powers with subtracted noise powers, i.e.,

$$Z_{DR} = 10\log[(P_h - N_h)/(P_v - N_v)] \quad \text{(dB)}. \tag{3}$$

The latter can be rewritten in the following form

$$Z_{DR} = 10\log[N_hN_v(P_h - N_h)/(P_v - N_v)\, N_hN_v] = SNR_h - SNR_v + 10\log(N_h/N_v)\,. \tag{4}$$

Z_{DRn} not corrected for noise is obtained as

$$Z_{DRn} = = SNR_{hn} - SNR_{vn} + 10\log(N_h/N_v)\,. \tag{5}$$

The difference between Z_{DR} and Z_{DRn} shows noise impact on Z_{DR} measurements.

2. WSR-88D KJIM

Fig. 2 presents response SNR curves for the IFD. The signal source was the signal generator Agilent 8648C (ID: F430162/5NXRAD). The noise impact on the not corrected SNR curves is noticeable at SNR less than about 10 dB (Fig. 2a). The noise corrected SNR curves are linear in an interval larger than 110 dB. Possible additional enlargement of this interval with linearization at very strong signals (the Sigmet invention) is not considered here because this linearization depends on the spectrum width and number of samples in the dwell time and it is not applicable for CW signals.

Fig. 2b shows deviations of noise corrected SNR (ΔSNR) from their linear dependence obtained for SNR larger than 50 dB. That straight line is extended to lower SNR. It is seen from Fig. 2b that the curves are close at SNR > 50 dB, but at lower SNR, they deviate by more than 0.1 dB. The latter means that Z_{DR}sys is not constant over the whole dynamic range and these deviations should be taken into considerations. Fig. 2c presents Z_{DR} curves obtained from noise corrected (the red curve) and not corrected (the blue curve) SNR. The measurements in the WSR-88Ds are conducted at SNR > 2 dB. At SNR > 2 dB, Z_{DR} experiences absolute deviations smaller than about 0.15 dB, i.e., the

channel mismatch in IFD can be larger than the desired 0.1 dB. Deviations between Z_{DR} and Z_{DRn} is larger than 0.1 dB at SNR less than 12 dB that points to the necessity of correcting SNR for noise at low SNR.

Time variations in ΔSNR and Z_{DR} (Fig. 3) during a day are less than 0.1 dB.

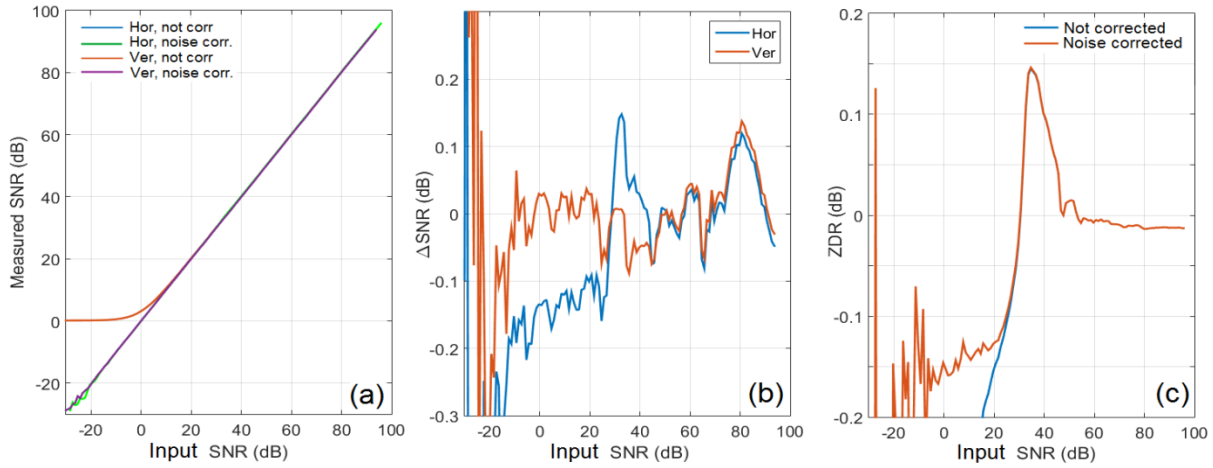

Fig. 2. KJIM. Dynamic curves at IF. June 6, 2018 at 18:30 UTC. (a): Dynamic curves for the not noise corrected SNR in the H- and V-channels (the blue and red curves; they practically coincide). The noise corrected dynamic curves are shown with the green and magenta lines. (b): Deviations from the linear parts of the dynamic curves for noise corrected SNR in the H- and V-channels. (c): Noise corrected Z_{DR} (the red curve) and Z_{DRn} not corrected for noise (the blue curve) obtained from (5).

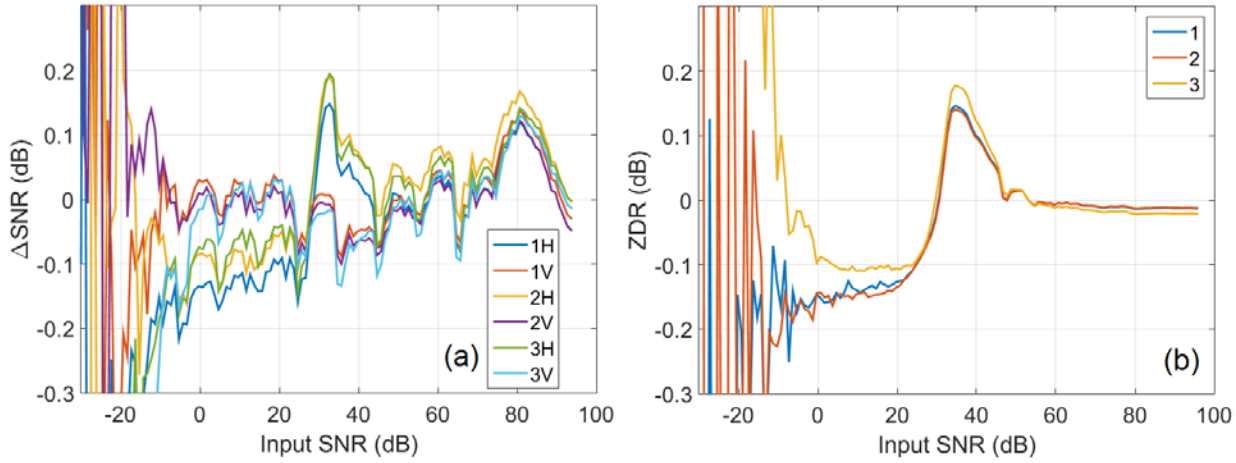

Fig. 3. KJIM. Dynamic curves at IF. 6 June, 2018. (a): ΔSNR for noise corrected SNR in the H- and V-channels. 1, 2, and 3 are results obtained at 1541, 1606, and 2056 UTC. (b): Noise corrected Z_{DR} obtained from curves in panel (a).

The next measurement step consists of determining the receive characteristics from the 30-dB RF directional couplers (Fig. 1) down to the signal processor RVP9. Fig. 4 shows the results obtained with the external calibrated signal generator Agilent 8648C. This generator's internal noise is small so that the dynamic curves at SNR < 0 dB

can be measured. It is seen that the dynamic curves in the channels exhibit a good match at SNR > 50 dB; at lower SNR the curves are not matched (Fig. 4b) and at about SNRs <~4 dB Z_{DR} bias can exceed 0.3 dB (Fig. 4c).

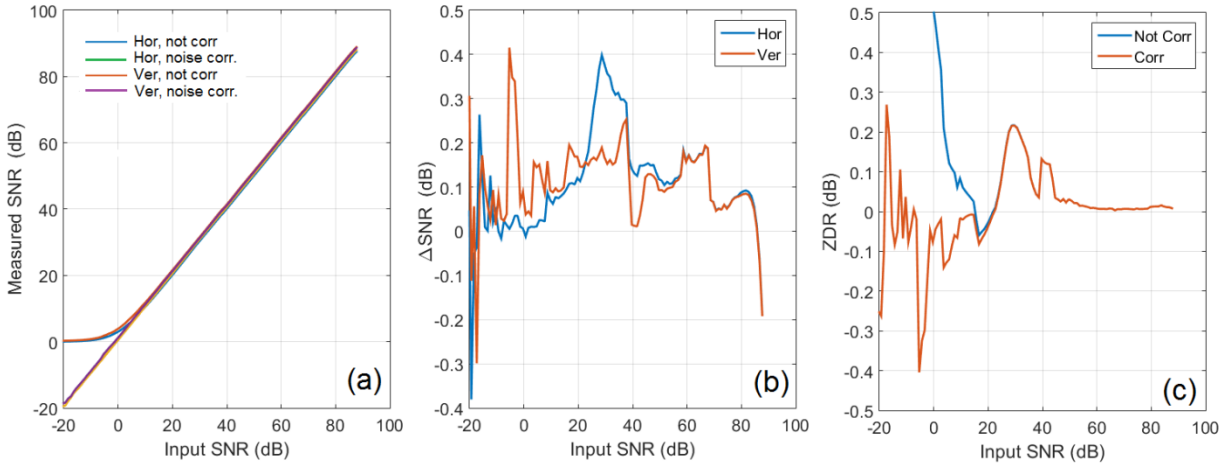

Fig. 4. KJIM. External RF calibrated signal generator. June 4, 2018 at 2127 UTC. The presentation format here is similar to the one in Fig. 2.

Comparing the curves in Figs.3b and 4c, we see that the large Z_{DR} peak exhibits about the same shape but is shifted horizontally. This offset is caused by the difference in input noise powers: the noise powers at the directional couplers are larger than that in the input to the IFD and the peak in Fig. 4c shifts to lower SNR. We can conclude that the IFD is mainly responsible for this peak.

The WSR-88D features a built-in calibration RF signal source. The dynamic curves obtained with this source are shown in Fig. 5. Our focus in sections 2-4 is on the variations of Z_{DR} with SNR. To show the impact of non-linearity of the dynamic curves, we shift measured Z_{DR} at SNR > 50 dB to 0 dB (Fig. 5c and similar figures). Therefore the Z_{DR} values from sections 2-4 should not be used for the estimation of Z_{DR} bias. Absolute Z_{DR} calibration is discussed in section 5.

One can see from Fig. 5a that with the built-in generator it is not possible to obtain the dynamic curve at low SNRs. Noise in the channels has been measured at the "isolated" attenuation switch's position. These noise levels were 0.73 and 0.76 dB higher than those measured in the H and V channels with the external generator's RF power off. This could cause a problem in obtaining the noise powers in the channels and in obtaining noise corrected SNR with the built-in signal source. The absolute variation in Z_{DR} with respect to 0 dB line (Fig. 5c) is about 0.2 dB as it was obtained with the external generator (Fig. 4c). Time variations of Z_{DR} can be seen in Fig. 6. Different values in the maximum of Z_{DR} in Fig. 6b could be due to different ambient temperatures: response '1' was obtained at 11^{o}C warmer temperature than response '2' because air conditioning in the radar shelter was down during the measurements.

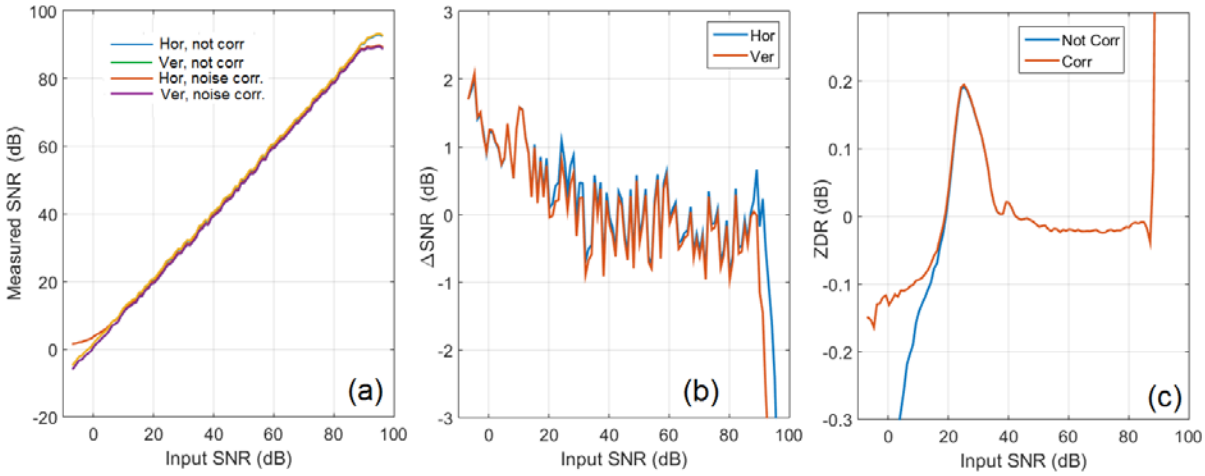

Fig. 5. KJIM. Built-in RF signal source. June 4, 2018 at 2003 UTC. The presentation format is similar to one in Fig. 4.

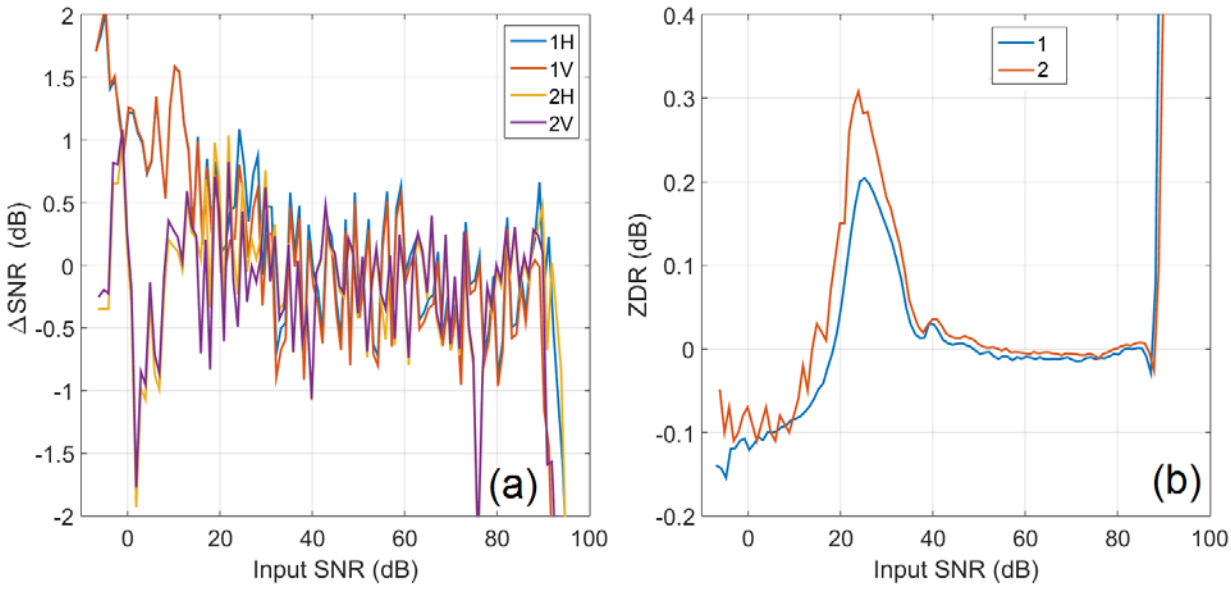

Fig. 6. KJIM. Built-in RF signal source. '1'is for June 4, 2018 at 2003 UTC, '2'is for June 6, 2018 at 1451 UTC.

3. WSR-88D KOUN

In the WSR-88 KOUN the IFD is located in the radar cabinet and is available for measuring its IF dynamic curves with an external signal generator. The RF Pallet is mounted on the antenna so only the built-in RF signal source is available for the measurements of RF dynamic curves.

Fig. 7 presents results of the dynamic curves measurements at IF, i.e., this is the dynamic curves of the IFD. Comparing Figs. 2 and 6 we note that the KOUN's IFD exhibits much less variations with SNR. The Z_{DR} variations (Fug. 7c) at SNR > 0dB are within the interval of ±0.05 dB, which is a very good performance, and is slightly higher that the Z_{DR} quantization interval. Fig. 8 is similar to Fig. 3 and shows time variations of the IFD dynamic curves, which are less than 0.05 dB over the course of 15 hours. The measurements were taken before the replacement the rotary joint in June 6, 2018.

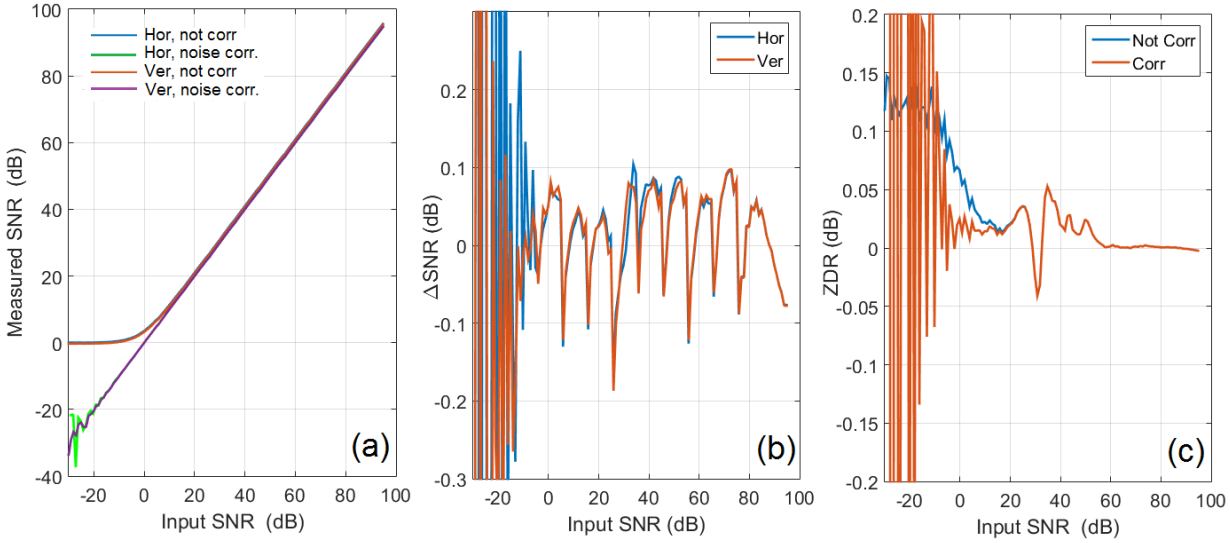

Fig. 7. KOUN. Dynamic curves at IF. Figure layout is as one in Fig. 2. May 13, 2018 at 0121 UTC.

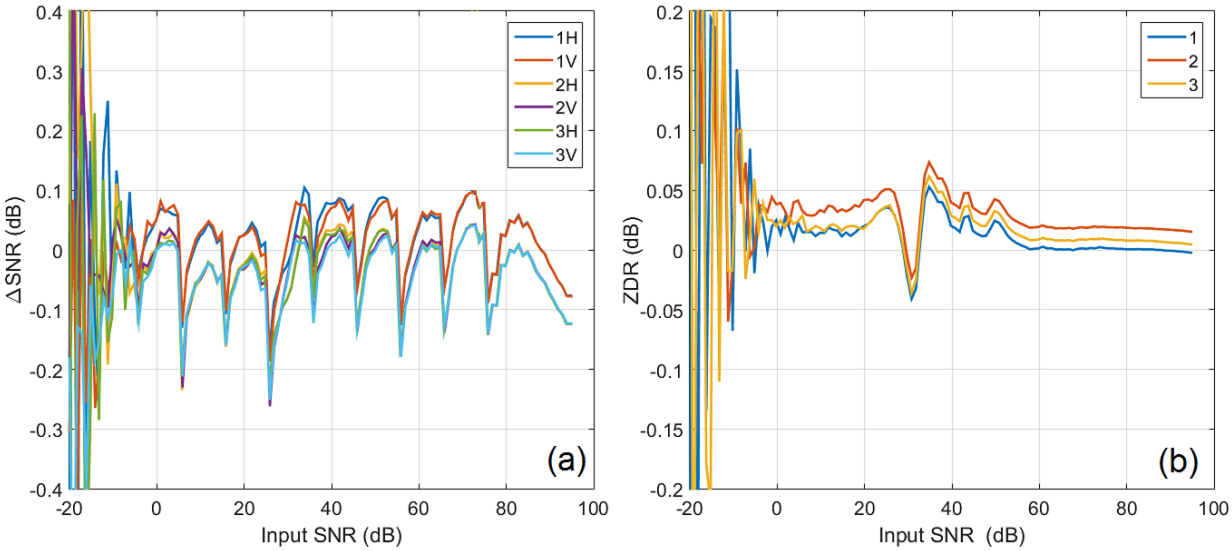

Fig. 8. KOUN. Dynamic curves at IF. Figure layout is as one in Fig. 3. June 13, 2018. '1' is for 0121 UTC, '2' is for 1450 UTC, and '3' is for 1517 UTC.

Fig. 9 presents the RF dynamic curves obtained with the built-in signal source. A problem with obtaining the noise power is seen in Fig. 9a, where the noise corrected dynamic curves drop sharply at negative SNR. It likely means overestimation of the noise powers that could be due to not complete isolation of the built-in signal source. One can see a big swing of the Z_{DR} curve (more than 0.6 dB, Fig. 9c) at SNR less than 30 dB. Time variations of the dynamic curves and Z_{DR} are shown in Fig. 10. The measurements show good temporal stability, but big variations at SNR < 30 dB.

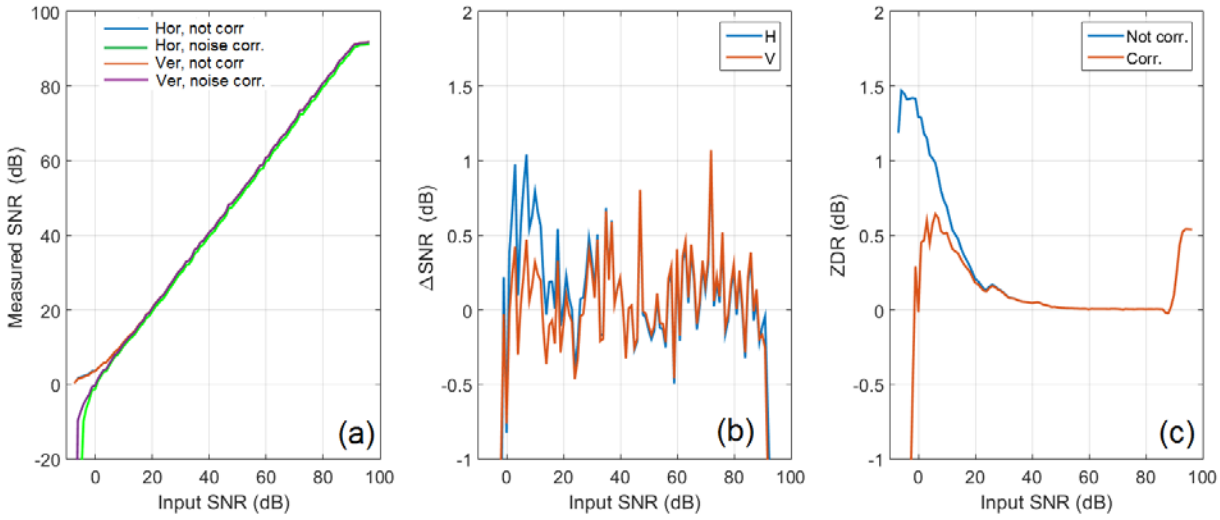

Fig. 9. KOUN. RF dynamic curves. Figure layout is as one in Fig. 5. May 14, 2018 at 2015 UTC.

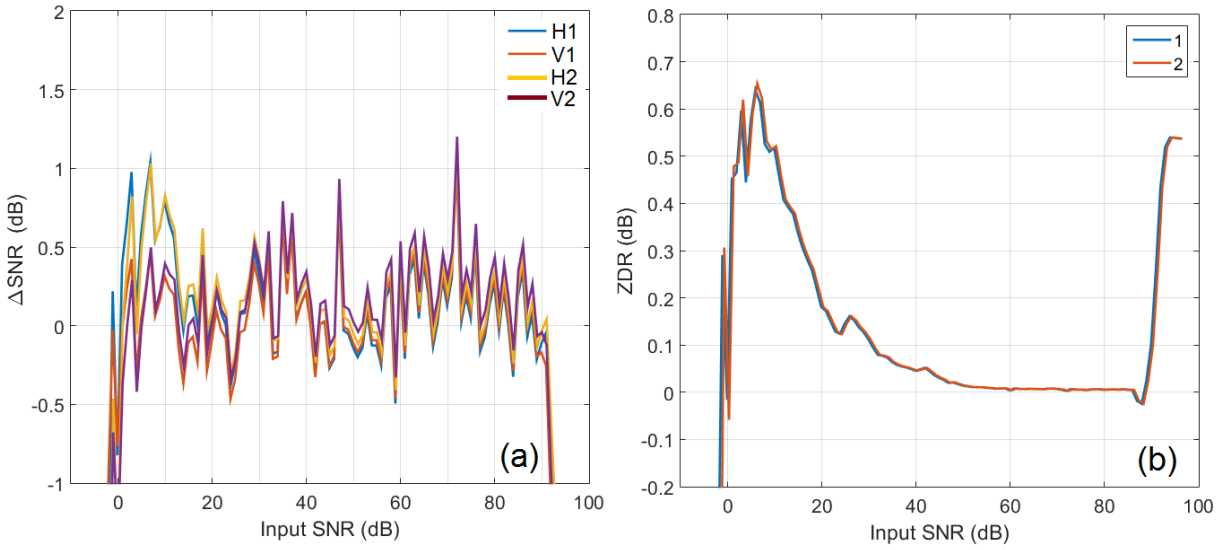

Fig. 10. KOUN. RF dynamic curves. Figure layout is as one in Fig. 6. '1'is for May 14, 2018 at 2015 UTC. '2' is for May 17, 2018 at 1956 UTC.

4. WSR-88D KREX

KREX was equipped with RVP8 signal processor at the time of the measurements. Fig. 11 presents results of the dynamic curves measurements at IF. The KREX's IFD exhibits variations in Z_{DR} of about 0.2 dB as functions of SNR (Fig. 11c). Time variations in IFD's Z_{DR} (Fig. 12b) are small over a course of about a month.

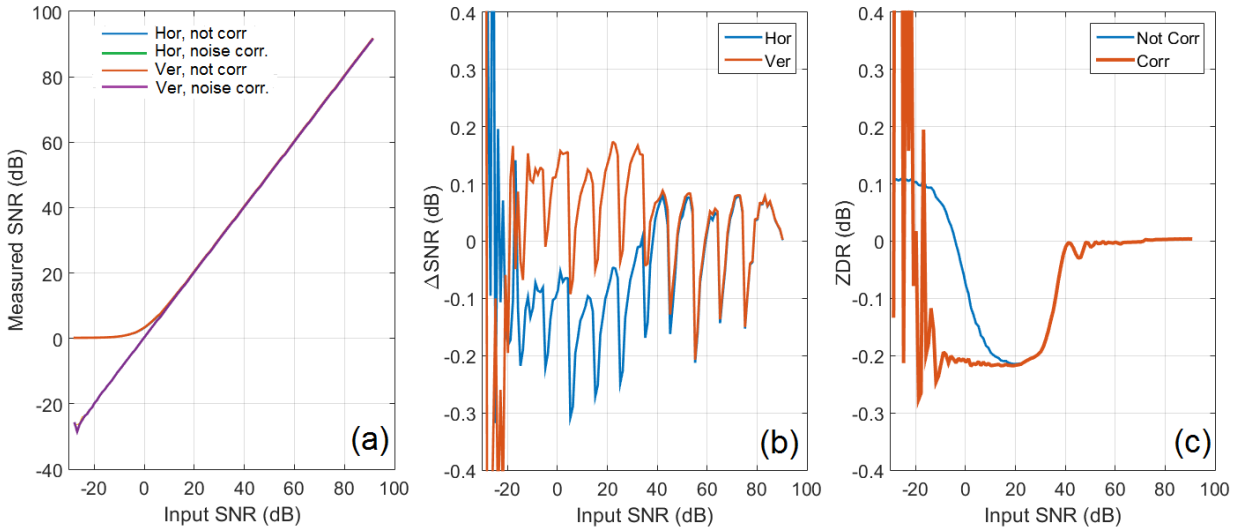

Fig. 11. KREX. Dynamic curves at IF. Figure layout is as one in Fig. 2. March 26, 2018 at 2054 UTC.

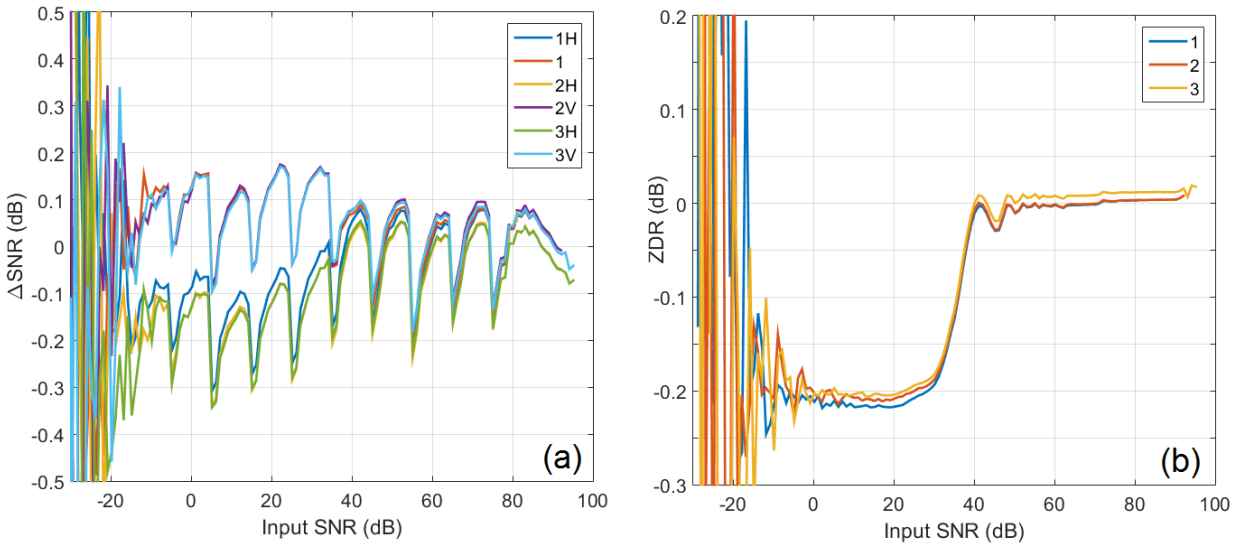

Fig. 12. KREX. Dynamic curves at IF. Figure layout is as one in Fig. 3. '1' is for March 26, 2018 at 2054 UTC. '2'is for April 3, 2018 at 2001 UTC. '3'is for April 16, 2018 at 2116 UTC.

RF Z_{DR} variations as a function of SNR (Fig. 13c) measured with the built-in signal source are about 0.1 dB. Because Z_{DR} should be calibrated with an accuracy of ±0.1 dB, these variations should be taken into account. Time variations in RF Z_{DR} (Fig. 14) are small.

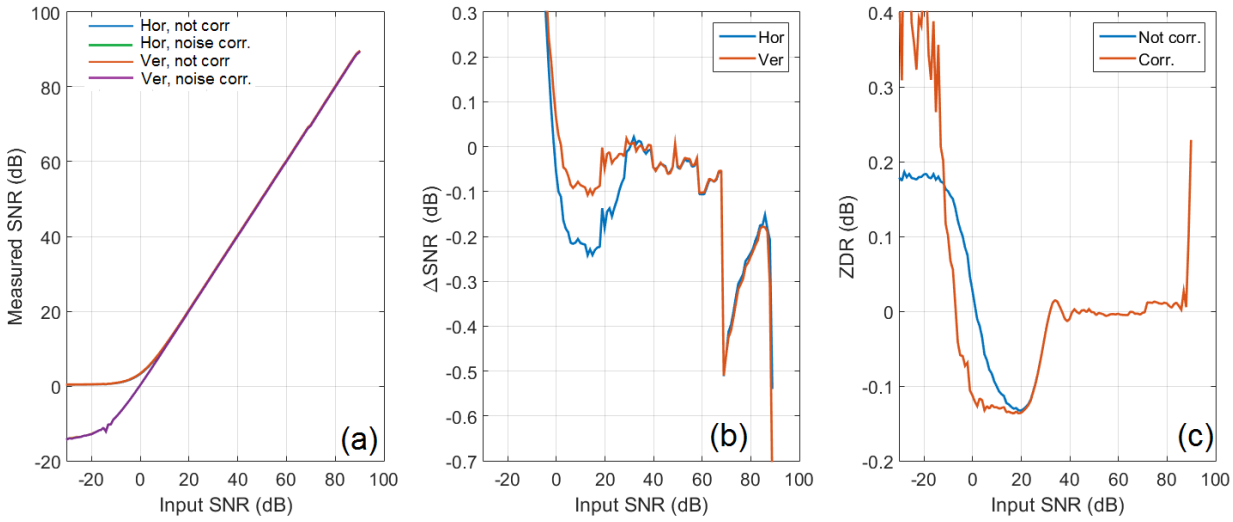

Fig. 13. KREX. RF dynamic curves. Figure layout is as in the one in Fig. 5. April 4, 2018 at 1904 UTC.

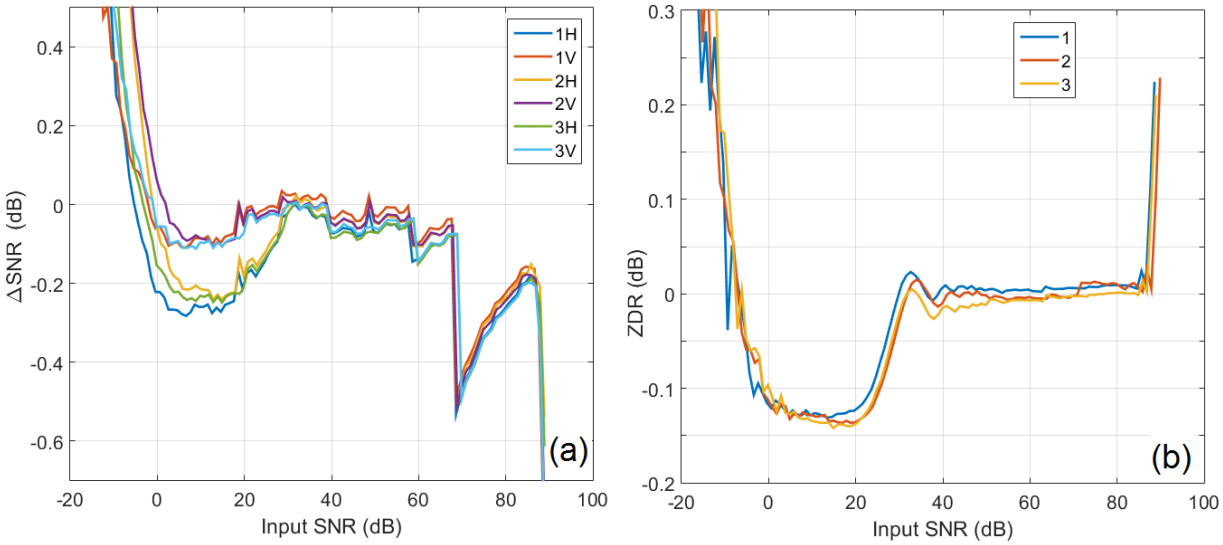

Fig. 14. KREX. RF dynamic curves. Figure layout is as one in Fig. 5. '1' is for May 1, 2018 at 1843 UTC. '2' is for April 30, 2018 at 1904 UTC. '3' is for May 2, 2018 at 1614 UTC.

5. Calibrating Z_{DR} on nonlinear receivers

The base line Z_{DR} calibration using the dedicated radar hardware consists of three routines: obtaining Z_{DR} offsets for the transmit and receive signal paths and measurements of solar flux's Z_{DR} to obtain the Z_{DR} offset of the antenna. Nonlinear receiver responses affect measurements of Z_{DR} offset in receive and antenna's Z_{DR}. In this section we

consider Z_{DR} calibration of the receive path beginning from the 30-dB couplers (Fig. 1). This is calibration of the receiver, i.e., the obtaining of RCB in the WSR-88D's calibration terms.

To calibrate Z_{DR} with an accuracy of 0.1 dB, nonlinearities of the dynamic responses as functions of SNR must be accounted for. RF Z_{DR} responses obtained in the previous sections for three WSR-88D radars cannot be directly used in Z_{DR} calibration because those responses have been obtained at certain input Z_{DR}. Since changes in input SNR have been made using a single attenuator at the signal generators (the internal built-in or external ones), the input Z_{DR} remained the same at various SNR levels. In operational practice, input Z_{DR} at S frequency band changes from about -5 dB (for almost vertically oriented ice crystals in thunderstorm or negative Z_{DR} due to differential attenuation in the channels) to 5 dB for large raindrops or hailstones with a toroidal water film. Ice clouds can have Z_{DR} up to 12 dB. This quite large Z_{DR} interval would require numerous dynamic curves obtained at various input Z_{DR} that would require hardware and software changes. Below we propose a different way to calibrate Z_{DR} not based on measurements of Z_{DR} responses. To demonstrate this approach, measurements on the WSR-88D KOUN are used.

By definition Z_{DR} is the ratio of signal powers S_h and S_v in the two polarization channels (see eq. (4)):

$$Z_{DR} = 10\log[(P_{in\text{-}h} - N_{in\text{-}h})/(P_{in\text{-}v} - N_{in\text{-}v})] \; . \tag{6}$$

The latter equation is written in a form to highlight that these quantities are ones at the input to the amplification hardware. At the output of the amplification hardware, i.e., in the RVP, the system produces $P_{out\text{-}h}$, $P_{out\text{-}v}$, $N_{out\text{-}h}$, and $N_{out\text{-}v}$. Amplification factors Q_h and Q_v in the channels (see below) must be obtained to recalculate the output quantities to the input ones to use (6). So the calibration procedure is the obtaining Q_h and Q_v for the whole receiver dynamic range. This can be accomplished with the existing radar hardware.

As it follows from the previous sections, responses Q_h and Q_v are not constant and depend on input powers, i.e., the receiver is not linear. By definition, Q_h and Q_v can be written as,

$$P_{out\text{-}h} = Q_h P_{in\text{-}h} \quad \text{and} \quad P_{out\text{-}v} = Q_v P_{in\text{-}v}. \tag{7}$$

Eq. (6) can then be rewritten as,

$$Z_{DR} = 10\log[Q_v Q_h(P_{in\text{-}h} - N_{in\text{-}h})/ Q_h Q_v(P_{in\text{-}v} - N_{in\text{-}v})] =$$

$$10\log[Q_v(Q_h P_{in\text{-}h} - Q_h N_{in\text{-}h})/ Q_h(Q_v P_{in\text{-}v} - Q_v N_{in\text{-}v})]. \tag{8}$$

Further,

$$Q_h P_{in\text{-}h} = P_{out\text{-}h} \; , \; Q_h P_{in\text{-}h} = P_{out\text{-}v} \; , \; Q_h N_{in\text{-}h} = N_{out\text{-}h}, \text{ and } Q_v N_{in\text{-}v} = N_{out\text{-}v}. \tag{9}$$

The noise powers in the channels are measured in range gates free from weather echoes, i.e., at lower signals than that corresponding to Q_h and Q_v in (8). Let Q_{hn} and Q_{vn} be amplifications at noise levels, then the measured noise powers $N_{h\text{-}meas}$ and $N_{v\text{-}meas}$ are:

$$N_{h\text{-}meas} = Q_{hn} N_{in\text{-}h} \quad \text{and} \quad N_{h\text{-}meas} = Q_{hn} N_{in\text{-}h} \; . \tag{10}$$

Substitution of $N_{in\text{-}h}$ and $N_{in\text{-}h}$ from the latter to (8) yields

$$Z_{DR} = 10\log[Q_v(Q_h P_{in\text{-}h} - Q_h N_{h\text{-}meas}/Q_{hn})/ Q_h(Q_v P_{in\text{-}v} - Q_v N_{in\text{-}v}/Q_{vn})] =$$

$$10\log[(P_{out\text{-}h} - N_{h\text{-}meas} Q_h/Q_{hn})/ (P_{out\text{-}v} - N_{v\text{-}meas} Q_v/Q_{vn})] + 10\log(Q_v/Q_h). \tag{11}$$

So, to calculate Z_{DR} from measured $P_{out\text{-}h}$, $P_{out\text{-}v}$, $N_{h\text{-}meas}$, and $N_{v\text{-}meas}$, the ratios Q_v/Q_h, Q_h/Q_{hn}, and Q_v/Q_{vn} should be known, i.e., measured, in whole dynamic range. The quantities in the first log in (11) are measured by the system

and the ratio Q_v/Q_h must be known for the given signal level. The obtaining of Q_v/Q_h is the receiver calibration procedure, which is discussed next. Once Q_v/Q_h is measured, the ratios Q_h/Q_{hn} and Q_v/Q_{vn} can be obtained. Fig. 16 presents Q_h - Q_v as functions of output SNR for the WSR-88D KOUN on two days.

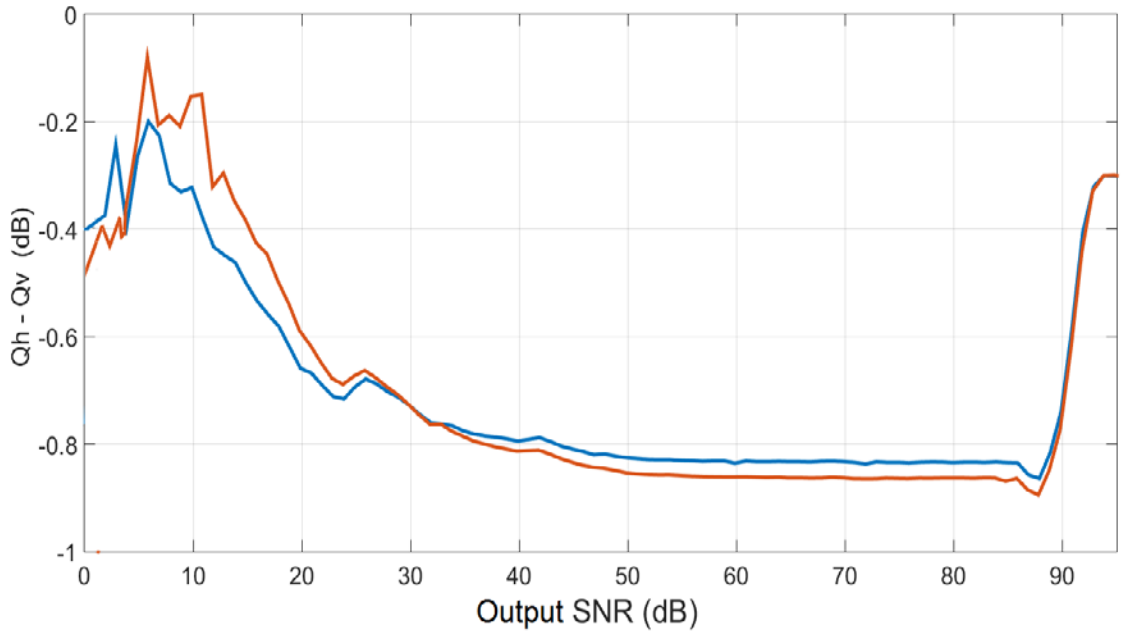

Fig. 16. Differences Q_h - Q_v as functions of output SNR. KOUN 14 May 2018 at 2015 UTC (blue curve) and 18 May 2018 at 1721 UTC.

6. Conclusions

An accuracy of Z_{DR} measurements of ±0.1 dB requires fine calibration, i.e., the system Z_{DR} offset needs to be measured with that accuracy. Typically, it is assumed that the system Z_{DR} offset is constant over the whole receiver dynamic range, i.e., the dynamic responses in the H and V channel differ by a certain value which is the Z_{DR} offset over the whole dynamic range. Measurements made on the WSR-88Ds shows that the dynamic responses are linear with an accuracy of ±1 dB which is sufficient for reflectivity measurements. For Z_{DR} measurements, the responses should be linear with an accuracy of ±0.1 dB. The measurement show that the receiver Z_{DR} offsets varies by 0.6 dB (KOUN, Fig. 10b), 0.3 dB (KJIM, Fig. 6b), and 0.1 dB (KREX, Fig. 14b) over the dynamic range. These variations have to be accounted for in the receiver Z_{DR} calibration.

Taking measurements with the built-in signal source, the noise level is obtained at the source switch position "isolated". This position could not give the true noise level because some signal could leak through. This issue could cause the increase in Q_h and Q_v curves at low SNR (Fig. 16). More study of this issue is needed.

Z_{DR} calibration for nonlinear receivers is described in section 5 and is based on measuring SNR responses in the channels. This approach does not use the Z_{DR} response curve but uses measured signal functions in the channels. The exact attenuation values of the 30-dB couplers (Fig. 1) and the powers of the built-in RF signal source are also needed for the calibration. These attenuation values are measured in the factory and are known for each system.

Some data suggest a temperature dependence of the receiver response (Figs. 6b and 16). If so, the dynamic receiver responses should be measured at various temperatures under the radome. If the receiver responses can be measured at the end of each VCP, i.e., there is sufficient time to take such measurements, the possible temperature dependence

is accounted for in the calibration because the current receiver responses Q_h and Q_v are obtained before the start of the next VCP.

Future work.

- A revision of the existing calibration procedure including RCB (receiver bias), TXB (transmitter bias), and SMB (antenna bias) contributions is needed by taking into account nonlinear receiver responses in the H and V channels. The nonlinear receiver is involved in the measurements of TXB and SMB as well and therefore affects these measurements.

- More study is needed to obtain the noise level of the built-in signal source. Conducted noise measurements could be biased by some signal leakage at the switch position "isolated". This leakage could be responsible for the increased values of $Q_h - Q_v$ at SNR < 30 dB (Fig. 16).

- Software should be designed to estimate needed time to measure the receiver responses Q_h and Q_v with a step of 1 dB over the whole dynamic range. A decision should be made on how frequently these measurements should be taken in operations, i.e., after each VCP if the required update time allows or less frequently otherwise.

Acknowledgements. We appreciate the help from Ms. Jane Krause, Mr. Glenn Secrest, and Mr. Randall Silver (all from the NWS Radar Operations Center) in collecting radar data during the course of this project.